Biochimica et Biophysica Acta 1842 (2014) 646–653

Contents lists available at ScienceDirect

Biochimica et Biophysica Acta

journal homepage: www.elsevier.com/locate/bbadis

Exogenous amyloidogenic proteins function as seeds in amyloid β-protein aggregation

Kenjiro Ono [a], Ryoichi Takahashi [a], Tokuhei Ikeda [a,b], Mineyuki Mizuguchi [c], Tsuyoshi Hamaguchi [a], Masahito Yamada [a,*]

[a] Department of Neurology and Neurobiology and Aging, Kanazawa University Graduate School of Medical Science, Kanazawa 920–8640, Japan
[b] Department of Neurology, National Hospital Organization Iou Hospital, Kanazawa 920–0192, Japan
[c] Faculty of Pharmaceutical Sciences, University of Toyama, 2630, Sugitani, Toyama 930–0194, Japan

ARTICLE INFO

Article history:
Received 13 November 2013
Received in revised form 12 December 2013
Accepted 7 January 2014
Available online 14 January 2014

Keywords:
Amyloid β-protein
Alzheimer's disease
Seeding effect

ABSTRACT

Amyloid β-protein (Aβ) aggregation is considered to be a critical step in the neurodegeneration of Alzheimer's disease (AD). In addition to Aβ, many proteins aggregate into the amyloid state, in which they form elongated fibers with spines comprising stranded β-sheets. However, the cross-seeding effects of other protein aggregates on Aβ aggregation pathways are not completely clear. To investigate the cross-seeding effects of exogenous and human non-CNS amyloidogenic proteins on Aβ aggregation pathways, we examined whether and how sonicated fibrils of casein, fibroin, sericin, actin, and islet amyloid polypeptide affected Aβ40 and Aβ42 aggregation pathways using the thioflavin T assay and electron microscopy. Interestingly, the fibrillar seeds of all amyloidogenic proteins functioned as seeds. The cross-seeding effect of actin was stronger but that of fibroin was weaker than that of other proteins. Furthermore, our nuclear magnetic resonance spectroscopic studies identified the binding sites of Aβ with the amyloidogenic proteins. Our results indicate that the amyloidogenic proteins, including those contained in foods and cosmetics, contribute to Aβ aggregation by binding to Aβ, suggesting their possible roles in the propagation of Aβ amyloidosis.

1. Introduction

Alzheimer's disease (AD) is characterized by the accumulation of amyloid plaques and neurofibrillary tangles. Amyloid β-protein (Aβ) is the primary component of amyloid plaques. Its aggregation is considered to be a critical step in the neurodegeneration of AD.

A nucleation-dependent model has been used to explain the mechanisms of Aβ aggregation *in vitro* [1,2]. This model consists of two phases, i.e., nucleation and extension. Nucleation requires a series of association steps of monomers that are thermodynamically unfavorable. Once the nucleus has been formed or the seed of Aβ fibrils (fAβ) has been added, further addition of monomers becomes thermodynamically favorable, resulting in the rapid extension of the amyloid fibrils [2,3]. Recent *in vivo* studies have reported exogenous induction of Aβ amyloidosis through intracerebral or peripheral administration of Aβ seeds in transgenic mice [4,5].

Other than Aβ, many proteins enter the so-called amyloid state, in which they form elongated fibers with spines comprising many stranded β-sheets. In some cases, cross-seeding between different amyloidogenic proteins occurs. We have shown that fibrils and oligomers of Aβ40, Aβ42, and α-synuclein (αS) affect the aggregation pathways acting as seeds among all species *in vitro* [6]. In addition, there are some reports of *in vitro* cross-seeding effect of different amyloidogenic proteins such as non-CNS amyloidogenic protein, islet amyloid polypeptide (IAPP), Aβ, αS, and tau [7–9]. Similarly, *in vivo* cross-seeding effect among heterologous, amyloidogenic proteins has also been reported [10].

Some of the proteins contained in cosmetics and food have been reported to be amyloidogenic. Through the use of cosmetics and intake of food, humans have been exposed to such exogenous amyloidogenic proteins. If the exogenous proteins function as seeds in Aβ aggregation pathways, they could contribute to the propagation of the Aβ amyloidosis and could be a possible risk for AD. Casein (Cas) is commonly found in mammalian milk, constituting up to 80% of the proteins in cow milk and between 20% and 45% of the proteins in human milk [11]. Cas also has a wide range of applications, including in cheese, as food additive, and a binder for safe matches [11]. Cas is natively unfolded in physiological conditions [12]. Cas monomers associate with each other to form colloidal aggregates (casein micelles), whereas, upon long duration of incubation at 37 °C, Cas, particularly α_{S2}-Cas, forms fibrils [12].

Fibroin (Fibro) and sericin (Ser) are two components of silk. Natural silk synthesized by the silkworm and spun in the form of a silk cocoon is originally synthesized in the silk gland. Silk proteins are important

Abbreviations: Aβ, amyloid β-protein; AD, Alzheimer's disease; Act, actin; αS, α-synuclein; Cas, casein; EM, electron microscopy; Fibro, fibroin; fAβ, Aβ fibrils; fAct, Act fibrils; fCas, casein fibrils; fFibro, fibroin fibrils; fIAPP, IAPP fibrils; fSer, sericin fibrils; HSQC, heteronuclear single quantum coherence; IAPP, islet amyloid polypeptide; NMR, nuclear magnetic resonance; Ser, sericin; ThT, thioflavin T

* Corresponding author. Tel.: +81 76 265 2290; fax: +81 76 234 4253.
E-mail address: m-yamada@med.kanazawa-u.ac.jp (M. Yamada).

0925-4439/$ – see front matter © 2014 Elsevier B.V. All rights reserved.
http://dx.doi.org/10.1016/j.bbadis.2014.01.002

bio-materials that have been used in the medical and cosmetic fields such as silk thread, complementary food, and cosmetic solution for external use because they show good compatibility with human tissues, oxidation resistance, antibacterial properties, and UV resistance [13]. The silk filament is a double strand of Fibro that is held together by a gummy substance called silk gum or Ser [14]. According to the nucleation-dependent model, Fibro converts to a β-sheet-enriched fibril structure [15]. Ser also easily changes from random coil to β-sheet structure [14].

Actin (Act) is one of the major proteins of the muscle system and cytoskeleton of non-muscle eukaryote cells such as algae [16]. The structure of Act is highly conserved. The differences between species are small; there is only 5% difference between the human and algae Act [16]. In the physiological state, Act polymerizes, forming the so-called fibrous form F-actin [17]. F-actin forms the backbone of thin filaments in muscle fibers [17].

IAPP is found in the amyloid deposits in the pancreas of 95% of the patients with type II diabetes and in a few other mammalian species, particularly monkeys and cats with diabetes [18]. IAPP is monomeric in its physiological state but is aggregated in the disease state. IAPP undergoes a multistep misfolding process in which the monomer changes into various oligomeric forms and ultimately forms fibrils [18].

The purpose of this study was to elucidate whether exogenous (Cas, Fibro, and Ser) as well as non-CNS amyloidogenic proteins (Act and IAPP) functioned as seeds in Aβ40 and Aβ42 aggregation pathways *in vitro*. Moreover, we analyzed the binding mechanism between Aβ and the above-described proteins using nuclear magnetic resonance (NMR) spectroscopy.

2. Materials and methods

2.1. Preparation of peptides

Aβ solutions were prepared as described previously [19]. Aβ40 and Aβ42 were purchased from the Peptide Institute Inc. (Osaka, Japan). Act from bovine muscle, Cas from bovine milk, and human IAPP were purchased from Sigma–Aldrich Co. LLC (St. Louis, MO). Fibro and Ser were purchased from Yousilk Ltd. (Kyoto, Japan) and Wako Pure Chemical Industries, Ltd. (Osaka, Japan), respectively. Peptide lyophilizates were dissolved at a concentration of 25 μM in 10% (v/v) 60 mM NaOH and 90% (v/v) 10 mM phosphate buffer, pH 7.4. After sonication for 1 min using a bath sonicator, the solutions were centrifuged for 20 min at 16,000 ×*g*.

2.2. Preparation of fibrils

The resulting supernatant was incubated at 37 °C for 2 (Aβ42) or 7 (Aβ40, Act, Cas, Fibro, IAPP, and Ser) days. After confirmation of each fibril formation by electron microscopy (Fig. 1), fresh fibrils were sonicated on ice with 30 intermittent pulses using an ultrasonic disruptor. These sonicated Aβ40 fibrils (fAβ40), Aβ42 fibrils (fAβ42), actin fibrils (fAct), casein fibrils (fCas), fibroin fibrils (fFibro), IAPP fibrils (fIAPP), and sericin fibrils (fSer) were used for the seeding assays.

2.3. Thioflavin T (ThT) binding

The reaction mixture contained 5 μM ThT (Wako Chemical Industries Ltd, Osaka, Japan) and 50 mM glycine–NaOH buffer, pH 8.5. After vortexing briefly, fluorescence was determined thrice at intervals of 10 s using a Hitachi F-2500 fluorometer. The excitation and emission wavelengths were 445 nm and 490 nm, respectively. Fluorescence was determined by averaging the three readings and subtracting the ThT blank.

2.4. Seeding activity of the fibrils of Aβ40, Aβ42, Act, Cas, Fibro, IAPP, and Ser

Fibrils of Aβ40, Aβ42, Cas, Fibro, Act, and Ser were prepared at a concentration of 25 μM in 10 mM phosphate buffer (pH 7.4). For the seeding assays, the sonicated fibrils were added to the un-aggregated peptides at a ratio of 10% (v/v) as seeds. The mixtures were incubated at 37 °C for 0–7 days.

2.5. Electron microscopy (EM)

A 10-μl aliquot of each sample was spotted onto a glow-discharged, carbon-coated formvar grid (Okenshoji Co. Ltd, Tokyo, Japan) and incubated for 20 min. The droplet was displaced with an equal volume of 2.5% (v/v) glutaraldehyde in water and incubated for an additional 5 min. Finally, the peptide was stained with 8 μl of 1% (v/v) uranyl acetate in water (Wako Chemical Industries Ltd). This solution was wicked off and then the grid was air-dried. The samples were examined using a JEM-1210 transmission electron microscope.

2.6. NMR spectroscopy

Lyophilized ^{15}N-labeled Aβ40 was dissolved in 50 mM NaOH on ice. The stock solution of Aβ40 was prepared by 10-fold dilution of the Aβ solution with 100 mM Tris-d_{11}, 1 mM NaN_3, and 10% D_2O (pH 7.4). NMR samples were prepared by 10-fold dilution of the stock Aβ40 solution with seeds solutions containing 10 mM phosphate and 10% D_2O (pH 7.0). The NMR sample of Aβ alone was prepared in the same manner without seeds. The final concentrations of Aβ40 and seeds were 60 μM and 45 μM, respectively. Spectra were obtained at 10 °C with a Bruker Avance 800 MHz spectrometer equipped with a cryoprobe (Bruker BioSpin, Rheinstetten, Germany). NMR data were processed with NMRPipe [20] and analyzed with NMRView [21]. The chemical shift perturbation (Δδ) was calculated by the equation,

$$\Delta\delta = \sqrt{(0.17\Delta^{15}\mathrm{N})^2 + (\Delta^{1}\mathrm{H})^2}, \quad (1)$$

in which Δ^{15}N represents the change in the chemical shift of the amide nitrogen and Δ^{1}H represents the change in the chemical shift of the amide proton [22].

2.7. Structural model of Aβ40

The atomic coordinate of Aβ40 was obtained from the Protein Data Bank (PDB ID: 2LFM) [23]. The regions of the structure showing a Δδ greater than 0.01 ppm and peak broadening were revealed on the model using the PyMol program (http://www.pymol.org/). These (backbone) regions were labeled in red.

2.8. Statistical analysis

One-way factorial analysis of variance (ANOVA) followed by the Tukey–Kramer *post hoc* comparisons were used to determine the statistical significance among the data sets. These tests were implemented within the GraphPad Prism software (version 4.0a, GraphPad Software, La Jolla, CA). Significance was defined as $p < 0.05$.

3. Results

3.1. ThT binding

To determine the effects of the fibrillar seeds on the peptide assembly, we used a well-characterized assay of fibril formation, the thioflavin dye binding [24]. As shown in Fig. 2A, when fresh Aβ40 was incubated at 37 °C, the ThT fluorescence followed a sigmoidal curve characterized by approximately 1-day lag time, approximately 5-day period of increasing

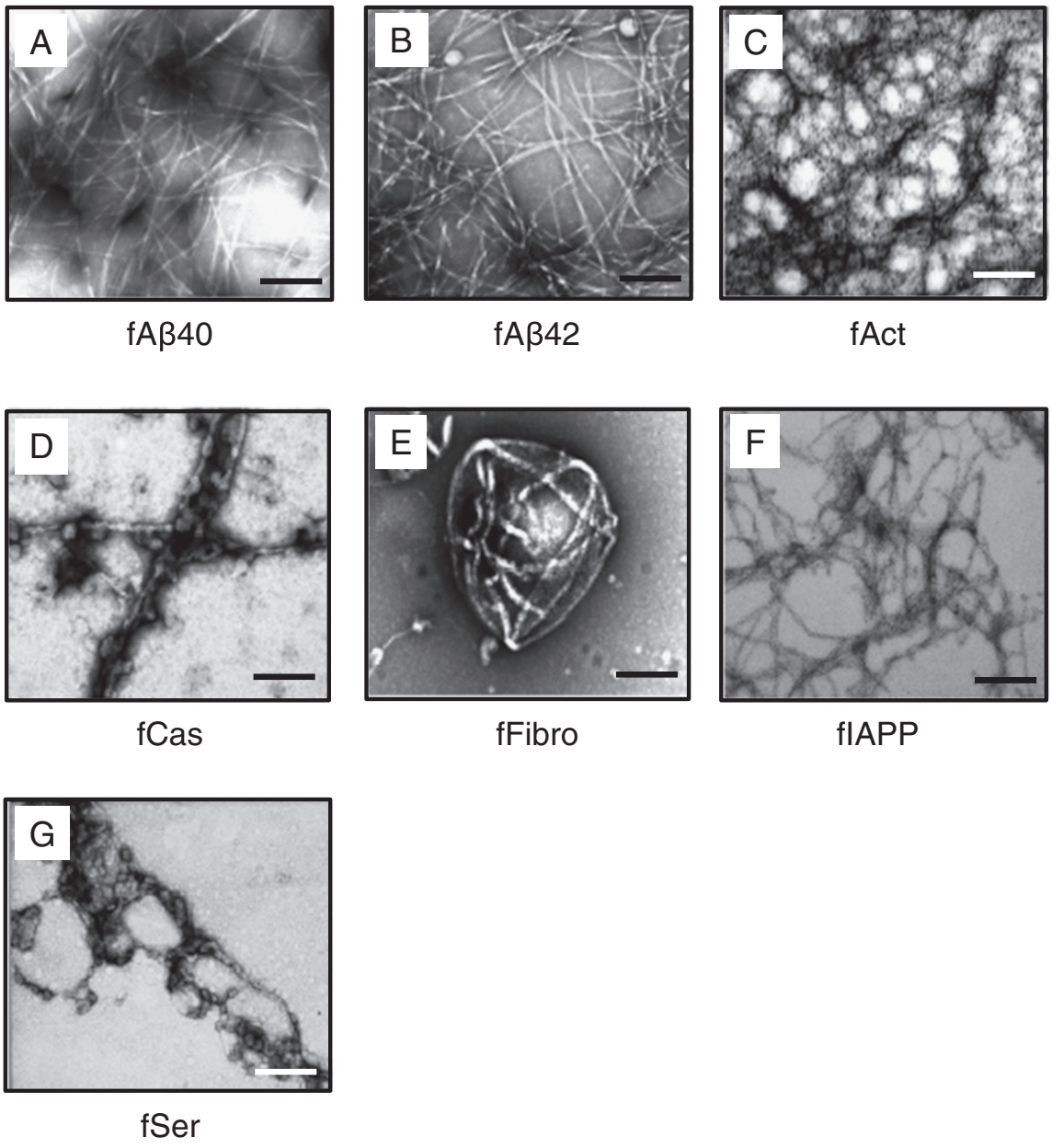

Fig. 1. EM morphologies of the fibrils of Aβ40 (fAβ40), Aβ42 (fAβ42), actin (fAct), casein (fCas), fibroin (fFibro), islet amyloid polypeptide (fIAPP), and sericin (fSer). The reaction mixtures containing 25 μM Aβ40 (A), Aβ42 (B), Act (C), Cas (D), Fibro (E), IAPP (F), or Ser (G), 10 mM phosphate buffer, pH 7.4, were incubated at 37 °C for 24 (B) or 168 (A, C–G) h. Scale bars indicate 100 nm.

ThT binding, and a plateau occurring after approximately 6 days. This curve is consistent with the nucleation-dependent polymerization model [1,19]. When fresh Aβ40 was incubated with fAβ40 at 37 °C, the fluorescence increased hyperbolically without a lag phase, and a plateau was reached after approximately 3 h (Fig. 2A). This curve is consistent with a first-order kinetic model [19]. The growth rate of fAβ40 was 59.2 FU/h. When fresh Aβ40 was incubated with fAct at 37 °C, the fluorescence also increased hyperbolically without a lag phase, and a plateau was reached after approximately 2 h (Fig. 2A). Similar seeding effects were observed after the addition of fCas, fFibro, fIAPP, or fSer, and the growth rates of fAct, fCas, fFibro, fIAPP, and fSer were 67.2, 49.0, 32.6, 51.7, and 54.0, respectively. The growth rate of fAct was bigger than the other rates ($p < 0.05$), whereas that of fFibro was smaller than the others ($p < 0.05$).

We obtained similar results with the assembly of Aβ42. As shown in Fig. 2B, when fresh Aβ42 was incubated at 37 °C, the ThT fluorescence followed a sigmoidal curve characterized by approximately 2-h lag time, approximately 10-h period of increasing ThT binding, and a plateau after approximately 12 h. When fresh Aβ42 was incubated with fAβ42 at 37 °C, the fluorescence increased hyperbolically without a lag phase, and the binding plateau occurred after approximately 2 h (Fig. 2B). The growth rate of fAβ42 was 59.7 FU/h. When fresh Aβ42 was incubated with fAct at 37 °C, the fluorescence also increased hyperbolically without a lag phase, and a plateau was reached after approximately 1 h (Fig. 2B). Similar seeding effects were observed after the addition of fCas, fFibro, fIAPP, or fSer, and the growth rates of fAct, fCas, fFibro, fIAPP, and fSer were 94.8, 60.8, 36.3, 61.9, and 72.4, respectively. The growth rate of fAct was bigger than the other rates ($p < 0.05$), whereas that of fFibro was smaller than the others ($p < 0.05$).

3.2. EM

We examined the fibrils morphologically. As shown in Fig. 1A, fAβ40 formed after the incubation of a fresh Aβ40 solution that assumed a

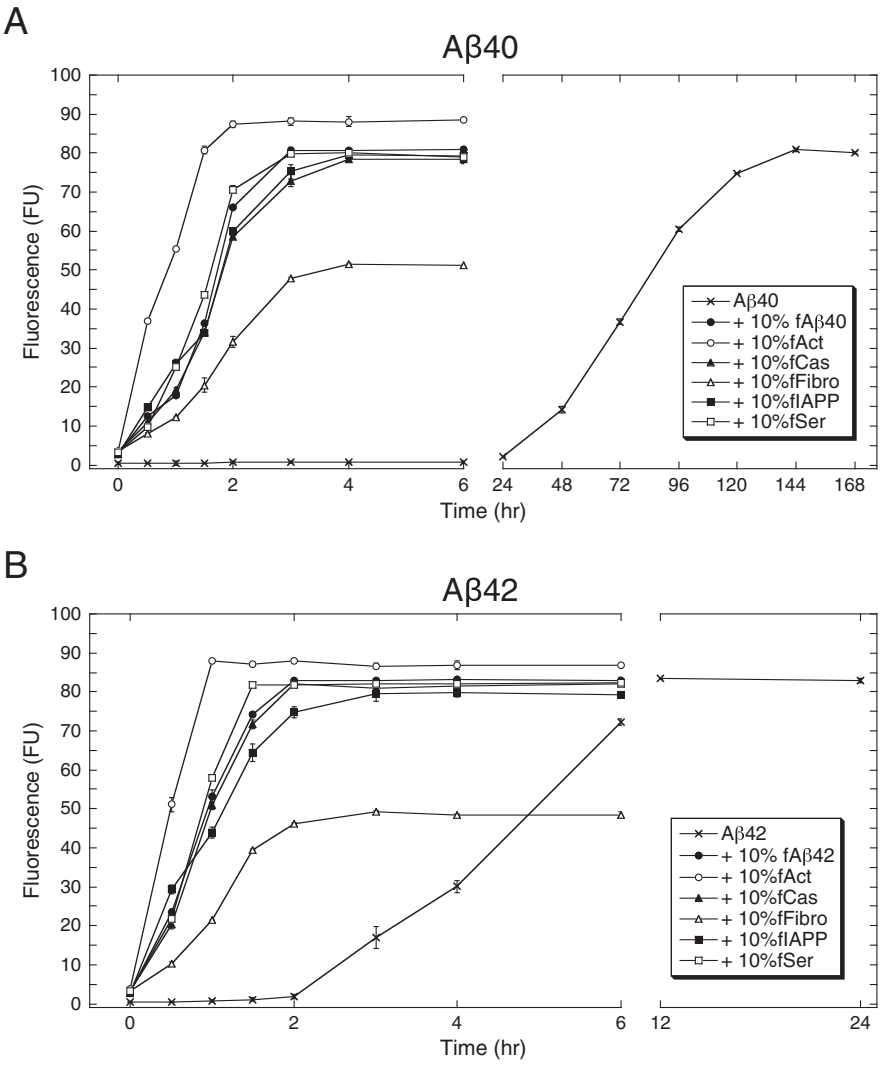

Fig. 2. Seeding effects of amyloid β-protein (Aβ), actin (Act), casein (Cas), fibroin (Fibro), islet amyloid polypeptide (IAPP), and sericin (Ser) in Aβ40 and Aβ42 aggregations. ThT binding. 25 μM Aβ40 (A) or Aβ42 (B) was incubated without (×) or with 10% (v/v) fAβ40 or fAβ42 (●), fAct (○), fCas (▲), fFibro (△), fIAPP (■), or fSer (□). Binding is expressed as mean fluorescence (FU) ± standard deviation (S.D.).

nonbranched, helical filament structure approximately 7-nm wide and exhibited a helical periodicity of approximately 220 nm, as described previously [19,25]. When Aβ40 was incubated with fAβ40 seeds (Fig. 3A), the typical fibrillar structure was also observed (Fig. 3B). Similarly, when Aβ40 was incubated with the seeds of fAct, fCas, fFibro, fIAPP, or fSer (Fig. 4A,D,G,J, and M), typical fibrillar structure was detected (Fig. 4B,E,H,K, and N). As shown in Fig. 1B, fresh Aβ42 solution formed a nonbranched filament of approximately 8 nm in width and with varying degrees of helicity, as described previously [19,25]. In addition, thicker, straight, non-branched filaments of approximately 12 nm width were observed. When Aβ42 was incubated with fAβ42 seeds (Fig. 3C), the typical fibrillar structure was observed (Fig. 3D). Similarly, when Aβ42 was incubated with the seeds of fAct, fCas, fFibro, fIAPP, or fSer (Fig. 4A,D,G,J, and M), the typical fibrillar structure was also detected (Fig. 4C,F,I,L, and O).

3.3. NMR studies

The binding between Aβ40 and the seeds was explored using NMR spectroscopy, a well-accepted tool for obtaining atomic-level information of protein–protein interactions. The low concentration of Aβ40 (60 μM) and low experimental temperature (10 °C) ensured that the Aβ40 remained monomeric during the entire data acquisition period [26]. Standard heteronuclear single quantum coherence (HSQC) spectra were obtained with uniformly ^{15}N-labeled Aβ40. The Aβ40:seeds ratio was maintained at a 1.3:1 molar ratio. The HSQC experiment detects ^{1}H signals that are directly bonded to the ^{15}N atoms, and thus provides a fingerprint of the amide-NH backbone atoms. The observed crosspeaks arise solely from monomeric Aβ40 [26].

Shown in Fig. 5 are the superimposed HSQC spectra of the Aβ40 (black crosspeaks) and the Aβ40 in the presence of seeds (Fig. 5, red crosspeaks). Because most of the crosspeaks of the superimposed spectra in Fig. 5 coincide, this indicates that the seeds do not affect the overall conformation of monomeric Aβ40. However, several crosspeaks in the presence of seeds showed small but significant NH chemical shift perturbation (labeled peaks in Fig. 5) indicative of binding. The significant movements ($\Delta\delta > 0.01$ ppm) corresponded to the E3, R5, H13, H14, Q15, K16, and L17 residues. Besides movements, NH peak broadening occurred with N27 in the presence of Aβ40 and actin seeds, suggesting that the N27 residue may be involved in the interaction with Aβ40 and actin seeds.

Highlighted in Fig. 6 are the molecular models of Aβ40 that show the binding locations in the presence of various seeds. In solution, the monomeric Aβ40 adopts a rapidly equilibrating ensemble of conformations that are predominately unstructured [27]. It is obvious that the seeds cause similar chemical shift changes in limited regions of Aβ40.

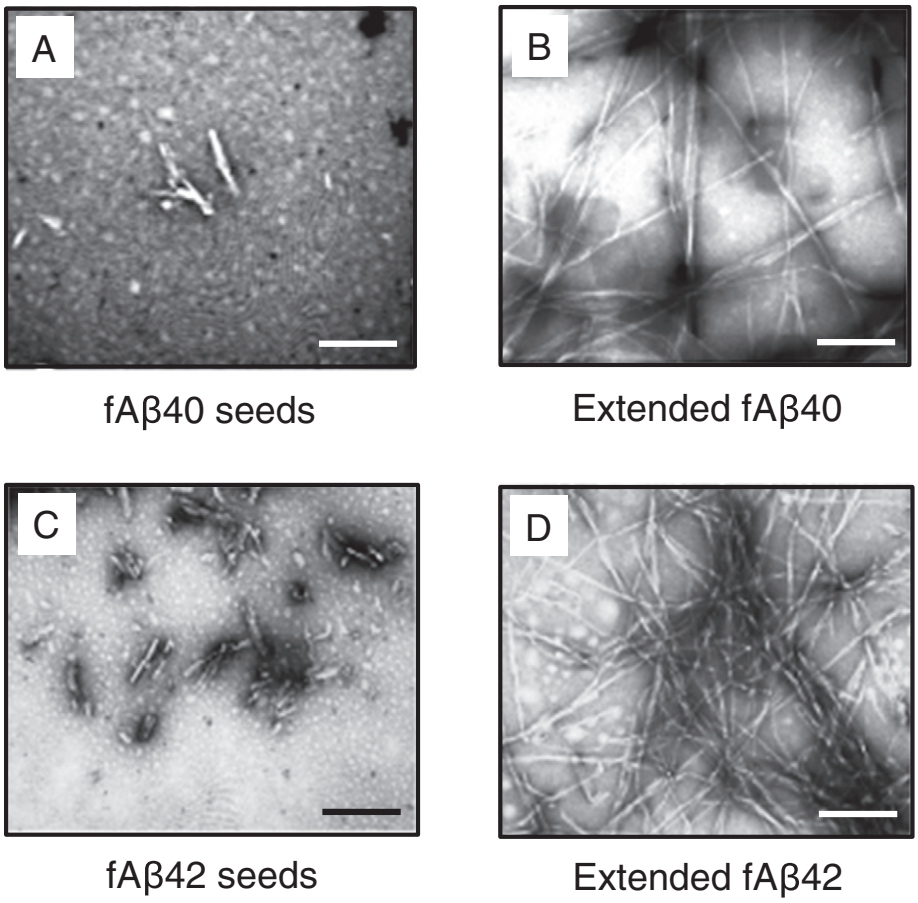

Fig. 3. EM morphologies of Aβ assemblies with fAβ seeds. The reaction mixtures containing 10 %(v/v) fAβ40 (A, B) or fAβ42 (C, D) seeds, 25 μM Aβ40 or Aβ42, 10 mM phosphate buffer, pH 7.4, were incubated at 37 °C for 0 (A, C), or 6 h (B, D). Scale bars indicate 100 nm.

4. Discussion

In this study, we focused on whether and how the fibrils of exogenous or non-CNS amyloidogenic proteins such as Act, Cas, Fibro, IAPP, and Ser influenced both Aβ40 and Aβ42 aggregation pathways as seeds *in vitro*. In the Aβ40 aggregation pathway, fAct, fCas, fFibro, fIAPP, and fSer as well as fAβ40 functioned as seeds. The activity of various seeds on the Aβ40 assembly was in the order of: fAβ40 = fAct > fCas = fIAPP = fSer > fFibro. Similarly, in Aβ42 aggregation pathway, fAct, fCas, fFibro, fIAPP, and fSer as well as fAβ42 functioned as seeds. Similarly, the activity of various seeds on the Aβ42 assembly was in the order of: fAβ42 = fAct > fCas = fIAPP = fSer > fFibro.

The molecular mechanism of the interaction between Aβ40, Aβ42, Act, Cas, Fibro, IAPP, and Ser needs to be considered. Previously, Naiki's group analyzed the interaction of Aβ40 and Aβ42 in the kinetics of the formation of fAβs *in vitro* using the ThT assay [28]. When fresh Aβ40 was incubated with fAβ42, the aggregation was accelerated by adding fAβ42 although the effect was much smaller than when fAβ40 was added to Aβ40 [28]. The fluorescence increased hyperbolically without a lag phase when Aβ42 was incubated with fAβ40, and proceeded to the equilibrium more rapidly than without fAβ40 [28]. The hydrophobic core of Aβ, i.e., residues 17–21, is reported to play an important role in the formation and stabilization of amyloid fibrils [29]. Remarkably, the sequences of IAPP and Aβ show 25% identity and 50% similarity [7]. It was reported that IAPP functions as seed in the aggregation of Aβ at the similar degree as 25–35 residues of Aβ although the seeding efficiency of IAPP was weaker than Aβ40 [7]. Beside the difference of the ratio of IAPP seed in the reaction, we could not have the appropriate explanation for this difference in the results. However, in our study, other proteins that do not have similar sequences exhibited the same seeding activity as IAPP in Aβ40 and Aβ42 aggregation. Interestingly, our NMR studies revealed that E3, R5, H13, H14, and Q15 of Aβ are common binding regions between the Aβ monomer and the fibrillar seeds of other proteins such as Act, Cas, IAPP, and Ser. These residues may electrostatically interact with other molecules. It was reported that a cluster of basic amino acids at the N-terminus (residues 13–16, HHQK), particularly H13, is critical for the interaction with glycosaminoglycan [30]. Similarly, it was reported that the HHQK region may bind to the membrane-associated heparin sulfate and microglial surfaces with high affinity [31,32]. We suggest that the common binding regions of Aβ may also recognize and interact with similar surface structures of different amyloidogenic protein seeds. Moreover, Act, which has the strongest seeding effect, and Aβ seeds bind with the same regions of the monomeric Aβ. Fibro, which has the weakest seeding effect, binds with fewer regions of the monomeric Aβ. The number of binding sites may also be an important factor for the seeding activity in the Aβ aggregation pathway.

The seeded proliferation of misfolded proteins that arose in prion disease holds considerable explanation for the pathogenesis of AD and other amyloidoses. Jucker's group showed that the phenotype of the induced Aβ deposits mirrors that of the deposits in the donor, suggesting an Aβ-templating mechanism [4,5]. Increasing evidence implicates the templated corruption of disease-specific proteins in other protein-misfolding diseases. A seeding-like process of αS lesions is bolstered by the observation that fetal dopaminergic neural transplants in the striatum of Parkinson's disease patients can eventually exhibit αS-positive Lewy bodies in some cells, implying that αS seeds propagate from the host to the graft [33,34]. Similarly, the induction of other protein aggregates such as superoxide dismutase 1 [35] and polyglutamine [36] has also been demonstrated in cell experiments.

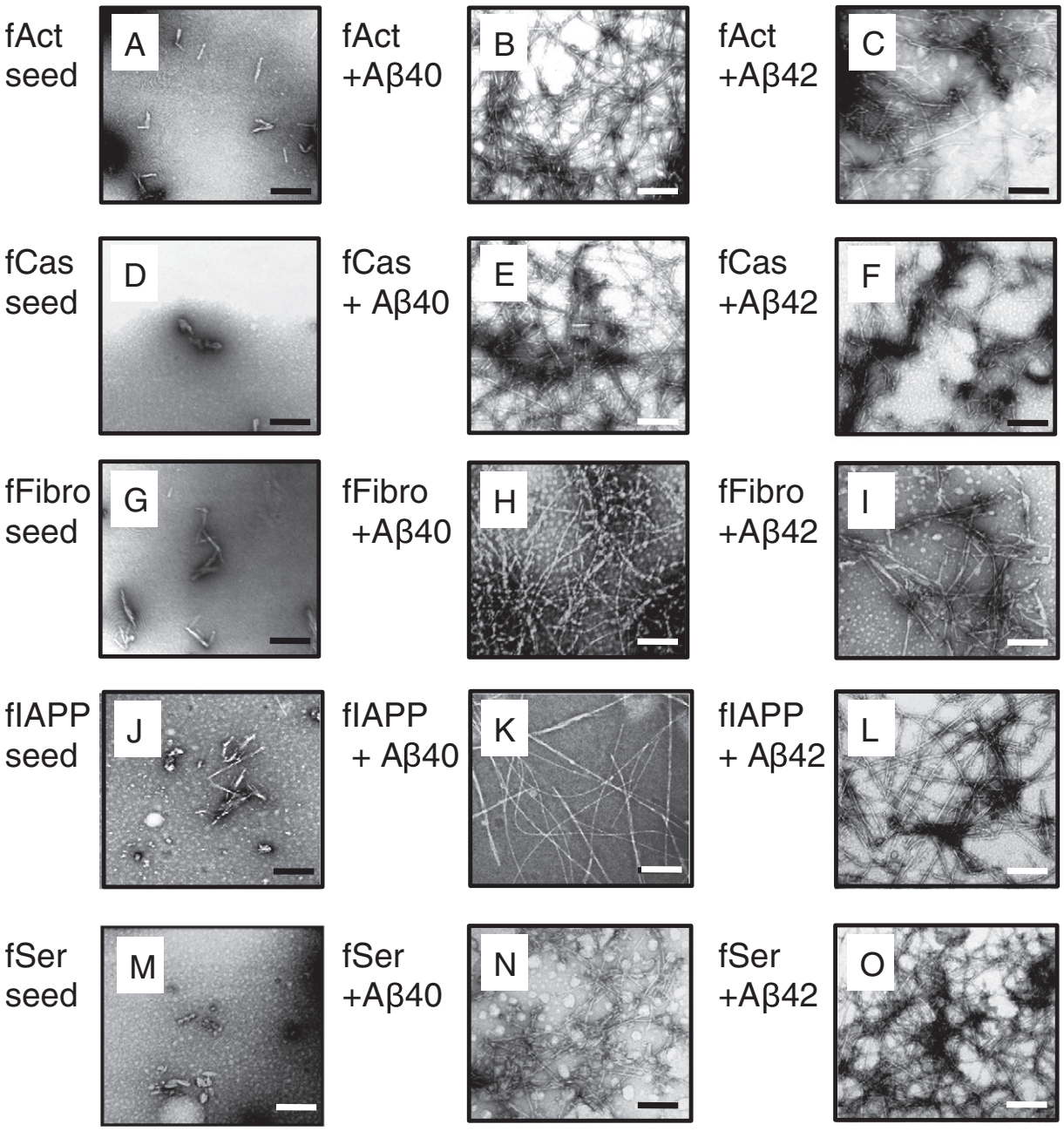

Fig. 4. EM morphologies of Aβ40 and Aβ42 assemblies with fibrillar seeds of amyloidogenic proteins. The reaction mixtures containing 10%(v/v) fAct (A–C), fCas (D–F), fFibro (G–I), IAPP (J–L) or fSer (M–O), 25 μM Aβ40 (B, E, H, K, N) or Aβ42 (C, F, I, L, O), 10 mM phosphate buffer, pH 7.4, were incubated at 37 °C for 0 (A, D, G, J, M), or 6 h (B, C, E, F, H, I, K, L, N, O). Scale bars indicate 100 nm.

Besides the *in vitro* cross-seeding of IAPP and Aβ [7], protein misfolding and aggregation can be initiated by heterologous, β-sheet-rich protein aggregates [8,9,37]. It was reported that αS aggregation was accelerated markedly by fibrillar seeds of the *Escherichia coli* chaperone in GroES, lysozyme, and insulin *in vitro* [8]. Furthermore, it was also reported that tau aggregation was promoted by the fibrillar seeds of αS in tau-expressing cells [9]. At the *in vivo* level, it was reported that the amyloid protein A amyloidosis was accelerated by the injection of synthetic fibrils of IAPP or transthyretin fragments in a mouse model [10]. At the human level, there was a report that a 28-year-old patient with iatrogenic Creutzfeldt–Jakob disease after dural grafting showed AD-type neuropathology such as senile plaques and cerebral amyloid angiopathy in widespread areas of the brain [38]. Plaque-type and vascular amyloid was immunohistochemically identified as deposits of Aβ [38], suggesting that Aβ pathology may be induced by the dura mater graft contaminated by prion or Aβ itself. Our results indicated that the seeds of exogenous amyloidogenic proteins, such as milk and silk proteins as well as non-CNS amyloidogenic proteins accelerate the Aβ aggregation pathway. These cross-seeding effects are generally less potent than homologous seeding. There have been no reports that the seeds of exogenous non-human, non-CNS amyloidogenic proteins, or their aggregates, enhance the Aβ burden in brain parenchyma of humans. Previously, we reported no significant correlations in amyloid deposition between the brain and non-CNS organs such as pancreas and heart in an autopsy series of AD and non-AD patients [39]. However, taken together with our results, the potential propagation of proteins by exogenous non-human nanoscale materials, some of which may feature amyloid-like structural properties [40,41], should be considered for careful evaluation. Further studies *in vivo* and in humans, including pathological investigations, are essential for clarifying the possible role

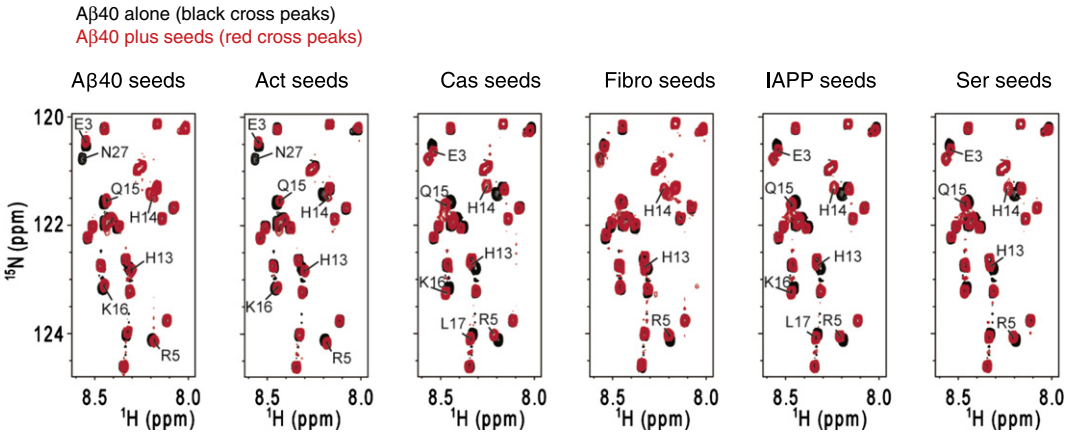

Fig. 5. Expanded ^{1}H–^{15}N HSQC spectra of Aβ40 in the absence of (black contour) and in the presence of (red contour) fibrillar seeds of Aβ40, Act, Cas, Fibro, IAPP, and Ser. Residues with $\Delta\delta > 0.01$ and the peak broadening are labeled.

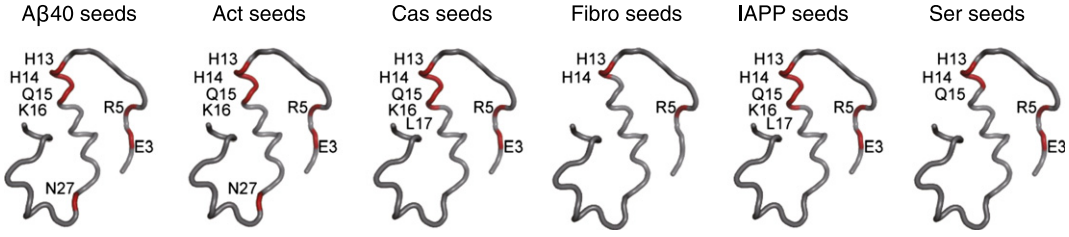

Fig. 6. Structural models of Aβ40 showing the binding locations with the fibrillar seeds of Aβ40, Act, Cas, Fibro, IAPP, and Ser. The atomic coordinate was obtained from the Protein Data Bank (PDB ID: 2LFM)[23]. The red-colored regions are residues that showed chemical shift changes and peak broadening in the presence of seeds.

of exogenous non-human or non-CNS amyloidogenic proteins in the propagation of cerebral Aβ amyloidosis.

In conclusion, the fibrils of amyloidogenic proteins, including exogenous proteins contained in food and cosmetics or non-CNS proteins, functioned as seeds in the Aβ aggregation pathway by binding to common regions of Aβ. Our results may provide new insights into the molecular mechanism of propagation of Aβ and other amyloidoses.

Acknowledgments

This work has been supported by Grants-in-Aid for Challenging Exploratory Research (22659170) (M.Y.), Scientific Research (B) (20390242) (M.Y.), Young Scientists (B) (K.O.), and Knowledge Cluster Initiative [High-Tech Sensing and Knowledge Handling Technology (Brain Technology)] (M.Y.) from the Japanese Ministry of Education, Culture, Sports, Science and Technology, Japan, a grant to the Amyloidosis Research Committee from the Ministry of Health, Labour, and Welfare, Japan (M.M., M.Y.), Novartis Foundation for Gerontological Research (K.O.), Takeda Science Foundation (K.O.), and Nagao Memorial fund (K.O.).

References

[1] J.T. Jarrett, P.T. Lansbury Jr., Seeding "one-dimensional crystallization" of amyloid: a pathogenic mechanism in Alzheimer's disease and scrapie? Cell 73 (1993) 1055–1058.
[2] A. Lomakin, D.S. Chung, G.B. Benedek, D.A. Kirschner, D.B. Teplow, On the nucleation and growth of amyloid β-protein fibrils: detection of nuclei and quantitation of rate constants, Proc. Natl. Acad. Sci. U. S. A. 93 (1996) 1125–1129.
[3] H. Naiki, K. Nakakuki, First-order kinetic model of Alzheimer's β-amyloid fibril extension in vitro, Lab. Invest. 74 (1996) 374–383.
[4] M. Meyer-Luehmann, J. Coomaraswamy, T. Bolmont, S. Kaeser, C. Schaefer, E. Kilger, A. Neuenschwander, D. Abramowski, P. Frey, A.L. Jaton, J.M. Vigouret, P. Paganetti, D.M. Walsh, P.M. Mathews, J. Ghiso, M. Staufenbiel, L.C. Walker, M. Jucker, Exogenous induction of cerebral β-amyloidogenesis is governed by agent and host, Science 313 (2006) 1781–1784.
[5] Y.S. Eisele, T. Bolmont, M. Heikenwalder, F. Langer, L.H. Jacobson, Z.X. Yan, K. Roth, A. Aguzzi, M. Staufenbiel, L.C. Walker, M. Jucker, Induction of cerebral β-amyloidosis: intracerebral versus systemic Aβ inoculation, Proc. Natl. Acad. Sci. U. S. A. 106 (2009) 12926–12931.
[6] K. Ono, R. Takahashi, T. Ikeda, M. Yamada, Cross-seeding effects of amyloid β-protein and α-synuclein, J. Neurochem. 122 (2012) 883–890.
[7] B. O'Nuallain, A.D. Williams, P. Westermark, R. Wetzel, Seeding specificity in amyloid growth induced by heterologous fibrils, J. Biol. Chem. 279 (2004) 17490–17499.
[8] H. Yagi, E. Kusaka, K. Hongo, T. Mizobata, Y. Kawata, Amyloid fibril formation of α-synuclein is accelerated by preformed amyloid seeds of other proteins: implications for the mechanism of transmissible conformational diseases, J. Biol. Chem. 280 (2005) 38609–38616.
[9] E.A. Waxman, B.I. Giasson, Induction of intracellular tau aggregation is promoted by α-synuclein seeds and provides novel insights into the hyperphosphorylation of tau, J. Neurosci. 31 (2011) 7604–7618.
[10] K. Johan, G. Westermark, U. Engstrom, A. Gustavsson, P. Hultman, P. Westermark, Acceleration of amyloid protein A amyloidosis by amyloid-like synthetic fibrils, Proc. Natl. Acad. Sci. U. S. A. 95 (1998) 2558–2563.
[11] C. Kunz, B. Lonnerdal, Human-milk proteins: analysis of casein and casein subunits by anion-exchange chromatography, gel electrophoresis, and specific staining methods, Am. J. Clin. Nutr. 51 (1990) 37–46.
[12] D.C. Thorn, H. Ecroyd, M. Sunde, S. Poon, J.A. Carver, Amyloid fibril formation by bovine milk αs2-casein occurs under physiological conditions yet is prevented by its natural counterpart, αs1-casein, Biochemistry 47 (2008) 3926–3936.
[13] X. Zhang, M. Tsukada, H. Morikawa, K. Aojima, G. Zhang, M. Miura, Production of silk sericin/silk fibroin blend nanofibers, Nanoscale Res. Lett. 6 (2011) 510.
[14] M.N. Padamwar, A.P. Pawar, A.V. Daithankar, K.R. Mahadik, Silk sericin as a moisturizer: an in vivo study, J. Cosmet. Dermatol. 4 (2005) 250–257.
[15] G. Li, P. Zhou, Z. Shao, X. Xie, X. Chen, H. Wang, L. Chunyu, T. Yu, The natural silk spinning process. A nucleation-dependent aggregation mechanism? Eur. J. Biochem. 268 (2001) 6600–6606.
[16] T.D. Pollard, L. Blanchoin, R.D. Mullins, Molecular mechanisms controlling actin filament dynamics in nonmuscle cells, Annu. Rev. Biophys. Biomol. Struct. 29 (2000) 545–576.
[17] O.I. Povarova, I.M. Kuznetsova, K.K. Turoverov, Physical-chemical properties of actin in different structural states. New ideas about its folding-unfolding pathways, Tsitologiia 47 (2005) 953–977.
[18] P. Westermark, A. Andersson, G.T. Westermark, Islet amyloid polypeptide, islet amyloid, and diabetes mellitus, Physiol. Rev. 91 (2011) 795–826.
[19] K. Ono, Y. Yoshiike, A. Takashima, K. Hasegawa, H. Naiki, M. Yamada, Potent anti-amyloidogenic and fibril-destabilizing effects of polyphenols in vitro:

implications for the prevention and therapeutics of Alzheimer's disease, J. Neurochem. 87 (2003) 172–181.
[20] F. Delaglio, S. Grzesiek, G.W. Vuister, G. Zhu, J. Pfeifer, A. Bax, NMRPipe: a multidimensional spectral processing system based on UNIX pipes, J. Biomol. NMR 6 (1995) 277–293.
[21] B.A. Johnson, Using NMRView to visualize and analyze the NMR spectra of macromolecules, Methods Mol. Biol. 278 (2004) 313–352.
[22] K.W. Lo, S. Naisbitt, J.S. Fan, M. Sheng, M. Zhang, The 8-kDa dynein light chain binds to its targets via a conserved (K/R)XTQT motif, J. Biol. Chem. 276 (2001) 14059–14066.
[23] S. Vivekanandan, J.R. Brender, S.Y. Lee, A. Ramamoorthy, A partially folded structure of amyloid-β(1–40) in an aqueous environment, Biochem. Biophys. Res. Commun. 411 (2011) 312–316.
[24] H. LeVine III, Quantification of β-sheet amyloid fibril structures with thioflavin T, Methods Enzymol. 309 (1999) 274–284.
[25] K. Ono, M.M. Condron, L. Ho, J. Wang, W. Zhao, G.M. Pasinetti, D.B. Teplow, Effects of grape seed-derived polyphenols on amyloid β-protein self-assembly and cytotoxicity, J. Biol. Chem. 283 (2008) 32176–32187.
[26] N.L. Fawzi, J. Ying, D.A. Torchia, G.M. Clore, Kinetics of amyloid β monomer-to-oligomer exchange by NMR relaxation, J. Am. Chem. Soc. 132 (2010) 9948–9951.
[27] L. Hou, H. Shao, Y. Zhang, H. Li, N.K. Menon, E.B. Neuhaus, J.M. Brewer, I.J. Byeon, D.G. Ray, M.P. Vitek, T. Iwashita, R.A. Makula, A.B. Przybyla, M.G. Zagorski, Solution NMR studies of the Aβ(1–40) and Aβ(1–42) peptides establish that the Met35 oxidation state affects the mechanism of amyloid formation, J. Am. Chem. Soc. 126 (2004) 1992–2005.
[28] K. Hasegawa, I. Yamaguchi, S. Omata, F. Gejyo, H. Naiki, Interaction between Aβ(1–42) and Aβ(1–40) in Alzheimer's β-amyloid fibril formation in vitro, Biochemistry 38 (1999) 15514–15521.
[29] S.J. Wood, R. Wetzel, J.D. Martin, M.R. Hurle, Prolines and amyloidogenicity in fragments of the Alzheimer's peptide β/A4, Biochemistry 34 (1995) 724–730.
[30] J. McLaurin, P.E. Fraser, Effect of amino-acid substitutions on Alzheimer's amyloid-β peptide-glycosaminoglycan interactions, Eur. J. Biochem. 267 (2000) 6353–6361.
[31] A.D. Snow, R. Sekiguchi, D. Nochlin, P. Fraser, K. Kimata, A. Mizutani, M. Arai, W.A. Schreier, D.G. Morgan, An important role of heparan sulfate proteoglycan (Perlecan) in a model system for the deposition and persistence of fibrillar Aβ-amyloid in rat brain, Neuron 12 (1994) 219–234.
[32] D. Giulian, L.J. Haverkamp, J. Yu, W. Karshin, D. Tom, J. Li, A. Kazanskaia, J. Kirkpatrick, A.E. Roher, The HHQK domain of β-amyloid provides a structural basis for the immunopathology of Alzheimer's disease, J. Biol. Chem. 273 (1998) 29719–29726.
[33] J.Y. Li, E. Englund, J.L. Holton, D. Soulet, P. Hagell, A.J. Lees, T. Lashley, N.P. Quinn, S. Rehncrona, A. Bjorklund, H. Widner, T. Revesz, O. Lindvall, P. Brundin, Lewy bodies in grafted neurons in subjects with Parkinson's disease suggest host-to-graft disease propagation, Nat. Med. 14 (2008) 501–503.
[34] J.H. Kordower, Y. Chu, R.A. Hauser, T.B. Freeman, C.W. Olanow, Lewy body-like pathology in long-term embryonic nigral transplants in Parkinson's disease, Nat. Med. 14 (2008) 504–506.
[35] C. Munch, J. O'Brien, A. Bertolotti, Prion-like propagation of mutant superoxide dismutase-1 misfolding in neuronal cells, Proc. Natl. Acad. Sci. U. S. A. 108 (2011) 3548–3553.
[36] P.H. Ren, J.E. Lauckner, I. Kachirskaia, J.E. Heuser, R. Melki, R.R. Kopito, Cytoplasmic penetration and persistent infection of mammalian cells by polyglutamine aggregates, Nat. Cell Biol. 11 (2009) 219–225.
[37] G.T. Westermark, P. Westermark, Prion-like aggregates: infectious agents in human disease, Trends Mol. Med. 16 (2010) 501–507.
[38] M. Preusser, T. Strobel, E. Gelpi, M. Eiler, G. Broessner, E. Schmutzhard, H. Budka, Alzheimer-type neuropathology in a 28 year old patient with iatrogenic Creutzfeldt-Jakob disease after dural grafting, J. Neurol. Neurosurg. Psychiatry 77 (2006) 413–416.
[39] M. Yamada, H. Tsukagoshi, E. Otomo, M. Hayakawa, Systemic amyloid deposition in old age and dementia of Alzheimer type: the relationship of brain amyloid to other amyloid, Acta Neuropathol. 77 (1988) 136–141.
[40] I. Cherny, E. Gazit, Amyloids: not only pathological agents but also ordered nanomaterials, Angew. Chem. Int. Ed. Engl. 47 (2008) 4062–4069.
[41] T.P. Knowles, M.J. Buehler, Nanomechanics of functional and pathological amyloid materials, Nat. Nanotechnol. 6 (2011) 469–479.